RSC Sustainability

ROYAL SOCIETY OF CHEMISTRY

PAPER

View Article Online
View Journal

Cite this: DOI: 10.1039/d6su00127k

The role of 2,3-butanediol stereochemistry in polyester synthesis

Marian Blom,[a] Robert-Jan van Putten,[ab] Bing Wang,[b] Gerard P. M. van Klink[ab] and Gert-Jan M. Gruter *[ab]

The shift toward sustainable platform chemicals enables the development of innovative, renewable polyesters that can potentially compete on performance. 2,3-Butanediol (2,3-BDO) is a monomer that can be produced from biomass and it can increase the glass transition temperature of the polyesters it is incorporated into. The use of biotechnological routes will generate either a pure form or a mixture of the 2,3-BDO stereoisomers. To assess potential differences in reactivity of these stereoisomers, several catalysts were tested in a model transesterification reaction of phenyl benzoate with *meso*- and *R*,*R*-2,3-BDO. After ~1 h, some catalysts, such as calcium acetate, did not show significantly different results in phenyl benzoate conversion between stereoisomer batches. Other catalysts, such as zirconium butoxide, showed higher yields when a batch of *R*,*R*-2,3-BDO was used. The opposite was observed for titanium butoxide, which showed more promising results for *meso*-2,3-BDO. Next, these zirconium and titanium butoxide catalysts were used for polymerization reactions with dimethyl terephthalate, resulting in similar trends for the different stereoisomers as was observed for the model reaction. The thermal degradation curves of the *meso*- and *R*,*R*-2,3-BDO-based terephthalate polyesters were similar, and no crystallinity was observed for either polyester. The catalysts La(acac)$_3$ and Zn(OAc)$_2$·2H$_2$O gave the highest yields in the transesterification model reaction. However, in polymer synthesis, both catalysts failed to reach the desired near-quantitative conversion with the commercial 2,3-BDO isomer mixture. Thus, the model transesterification reaction cannot be used to predict performance in polymer synthesis, but it can provide useful insight into performance trends related to 2,3-BDO stereochemistry.

Received 1st March 2026
Accepted 19th May 2026

DOI: 10.1039/d6su00127k

rsc.li/rscsus

Sustainability spotlight

Shifting to renewable materials is essential for reducing the carbon footprint of fossil plastics. Polyesters offer benefits because they can be prepared with much better atom efficiency than polyolefins from biomass and CO_2 and they can be closed-loop recycled both chemically and mechanically. 2,3-Butanediol is an interesting sustainable bio-based monomer which has three stereoisomers (*meso*, *R*,*R*, and *S*,*S*). Different biotechnological production options will generate specific stereoisomer ratios which differ from fossil-based 2,3-butanediol. How these stereoisomers behave in polyester synthesis is important for the production of their polyesters. Renewable polyesters with enhanced properties such as higher glass transition temperatures and better barriers allows competition on performance instead of on price as is the case for drop-in bio-PET, bio-PE, *etc.* UN sustainable development goals: industry, innovation, and infrastructure (SDG 9), responsible consumption and production (SDG 12) and climate action (SDG 13).

Introduction

Using sustainable platform chemicals is essential for decreasing our reliance on fossil fuels. Additionally, these building blocks present an opportunity to develop innovative renewable materials that can potentially compete on performance. Poly(lactic-*co*-glycolic acid) can be made from sustainable resources and has excellent barrier properties.[1] Additionally, isosorbide-based polyoxalates (PISOXs) are biodegradable high-performance materials derived from CO_2- or bio-based monomers.[2] Another example is the sugar-based 2,5-furandicarboxylic acid (FDCA) used in PEF, a high barrier material.[3]

Improved properties would enable these renewable polyesters to gain market share, as it is challenging to compete on price alone with the scale difference and the highly optimized production of fossil-based polymers. For example the incorporation of isosorbide (IS), a bicyclic secondary diol, in PISOX resulted in a relatively high glass-transition temperature (T_g), thereby improving the potential applicability of the product by expanding its temperature range of usage.[2]

While secondary diols, like sugar-based IS, are known to increase the T_g, they have less reactive hydroxyl groups, leading

[a]*Industrial Sustainable Chemistry, van't Hoff Institute of Molecular Sciences, University of Amsterdam, Science Park 904, 1098 XH Amsterdam, The Netherlands. E-mail: G.J.M.Gruter@uva.nl*

[b]*Avantium Support B.V., Zekeringstraat 29, 1014 BV Amsterdam, The Netherlands*

to longer reaction times and/or lower degrees of polymerization.[4] To address these issues, novel synthesis strategies have been developed to incorporate IS. Using reactive solvents allows for high $\bar{M}_n$ polymers based on IS.[5] Employing a "traceless" linker for furanoate copolymers of IS and EG significantly shortens reaction times without requiring additional metal catalysts.[6]

Not all renewable secondary diols have been as thoroughly studied as IS, which is also the case for 2,3-butanediol (2,3-BDO). Consequently, polymers based solely on this diol, 2,3-BDO, have number-average molecular weight ($\bar{M}_n$) values below 20 kDa and require long reaction times for their synthesis.[7–11] This is due to the low reactivity of 2,3-BDO, which under certain conditions can be six to ten times lower than that of the linear primary 1,4-butanediol.[12] To still obtain a high conversion in a shorter time span, the use of a more efficient catalyst could be a solution, yet a balance should be found between the environmental impact of the catalyst and its effectiveness to realize more sustainable production.

Titanium, tin and germanium-based catalysts have been used in the synthesis of 2,3-BDO-based polyesters.[9,10,13–15] However, it is possible that these are not the most effective catalysts. For instance, Kirchberg *et al.* reported that iron(III) chloride outperformed titanium(IV) isopropoxide (TTIP) in the synthesis of poly(2,3-butylene furanoate), based on the resulting molecular weights.[7] In this study, the deconvolution method was used to screen several catalysts at once. The two step polymer synthesis consisted of direct esterification followed by polycondensation. Mixtures of four different catalysts were used with a total catalyst loading of 4 mol%. While this approach gives fast results, it does not fully reflect the individual performance of each catalyst. Factors such as catalyst intoxication by impurities, presence of several mol% ligands, metal–metal interactions, and side reactions could significantly influence both individual catalytic activity and the maximum achievable $\bar{M}_n$ of the product. Moreover, catalyst performance can vary depending on the reaction stage of the polymerization. Despite this, the screening successfully identified a high-performing catalyst, iron(III) chloride, which is both cost-effective and environmentally friendlier than other established catalysts. The use of chlorides could, however, lead to issues in future upscaling in steel reactors, because of their corrosive properties.

Another aspect to consider when using renewably sourced monomers is that they may differ from fossil-based products due to the presence or absence of various impurities or catalyst traces. In the case of 2,3-BDO, an additional factor is its stereoisomeric nature, as it can occur in three stereoisomeric forms: *meso*-2,3-BDO, *R*,*R*-2,3-BDO and *S*,*S*-2,3-BDO. The *S*,*S*- and *R*,*R*-forms are mirror images and therefore have identical reactivity. Fossil-based 2,3-BDO typically contains a mixture of all three stereoisomers, whereas renewable pathways can yield a single stereoisomer or different unique isomer mixtures.[16] Shen *et al.* found that the meso isomer has a lower gas phase basicity compared to the other stereoisomers.[17] This suggests that the reactivities of the isomers might differ, but based on the gas phase data alone it is not possible to determine whether this has any significant influence on polymerization reactions. The most relevant work was published in 1951 by Ripley and Watson on the ring opening polymerization of a six-membered ring derived from 2,3-BDO and oxalate.[18] They reported that the ring based on *meso*-2,3-BDO had markedly better performance than the one based on *R*,*R*-2,3-BDO, particularly in the presence of a catalyst. This may be attributed to differences in ring strain between the different stereoisomeric forms of the starting material, or to other contributing factors. This demonstrates that stereochemistry has an influence; however, it does not offer a clear indication of its impact on the conventional (non-ring-opening) transesterification. Understanding the effect of the use of a specific 2,3-BDO stereoisomer on transesterification is crucial, as it may influence the polyester synthesis time and/or the temperature required to achieve sufficiently high molecular weights.

Additionally, the stereochemistry of the monomer (*meso*, *R*,*R*, or *S*,*S*) may lead to notable differences in polymer properties, such as crystallinity, which in turn affects its suitability for specific applications. A lack of crystallinity can enhance clarity, and the resulting absence of a melting point can be either advantageous or disadvantageous, depending on the specific use case. Glycol-modified PET (PETG) is often used in applications requiring amorphous polymers. The use of 2,3-BDO for polyesters is being explored to create a material similar to "on-the-market PETG" but with a higher T_g.[9,10] In these studies, 2,3-BDO is combined with a codiol and dimethyl terephthalate (DMT) in a transesterification reaction followed by a polycondensation step, which is similar to the method historically used for the production of PET.

Before 2,3-BDO can be used as a high T_g polymer building block, a better understanding of its reactivity is needed to further optimize its use in polymer synthesis. This study primarily focuses on the initial step of polymer synthesis and tries to elucidate what influence the stereoisomer composition of 2,3-BDO has on the transesterification. Therefore, *meso*- and *R*,*R*-2,3-BDO were evaluated in a model transesterification reaction using several conventional catalysts. Since the *S*,*S*-form is expected to have the same reactivity as the *R*,*R*-form (unless the environment is chiral) this stereoisomer was not tested. All these stereoisomers can be produced *via* biotechnological routes.[16,19–21] The most outstanding performances observed in the model reaction were applied at a larger scale for polymer synthesis using dimethyl terephthalate. Furthermore, the relevant effects of using specific 2,3-BDO stereoisomers on the properties of these polymers, such as crystallinity, were analysed.

Experimental

Materials

All listed starting materials, catalysts and solvents were used as received. Phenyl benzoate (99.95%, BLD Pharmatech), *R*,*R*-2,3-butanediol (99.07%, BLD Pharmatech), *meso*-2,3-butanediol (99%, Sigma-Aldrich), titanium(IV) *n*-butoxide ($Ti(OBu)_4$) (97%, Sigma-Aldrich), ytterbium(III) trifluoromethanesulfonate ($Yb(OTf)_3$) (99.99%, Sigma-Aldrich), *p*-toluenesulphonic acid monohydrate (*p*-TSA) (99%, Acros Organics), lanthanum(III)

acetylacetonate hydrate ($La(acac)_3$) (27.3–23.4% La, Sigma-Aldrich), zirconium(IV) *n*-butoxide ($Zr(OBu)_4$) (80% w/w in 1-butanol, ThermoFisher), calcium acetate monohydrate ($Ca(OAc)_2 \cdot H_2O$) (ACS reagent ≥99%, Sigma-Aldrich), zinc acetate dihydrate ($Zn(OAc)_2 \cdot 2H_2O$) (99.0–101.0%, Alfa Aesar), antimony(III) oxide (Sb_2O_3) (ReagentPlus 99%, Sigma-Aldrich), butyltin hydroxide oxide hydrate ($CH_3(CH_2)_3Sn(=O)OH \cdot xH2O$) (97%, Sigma-Aldrich), dimethyl terephthalate (DMT) (99%, ThermoFisher), 2,3-BDO (98%, Sigma-Aldrich, *meso* : *R*,*R* ratio of 78 : 22 based on H^1-NMR spectrum), chloroform-d ($CDCl_3$) (99.8% D and 99.8% D containing 1 v/v% TMS, Sigma-Aldrich), and dichloromethane (DCM) (stab. 0.002% 2-methyl-2-butene, VWR international).

Transesterification of phenyl benzoate in HPLC vials

Phenylbenzoate (PhOBz) (1190 mg, 6 mmol, 1 eq.), *meso*- or *R*,*R*-2,3-BDO (270 mg, 3 mmol, 0.5 eq.), and the catalyst (0.02 mmol, 0.0032 eq.) were added to an HPLC vial (5 cm height, 16 mm diameter). The amounts used may vary slightly between reactor vials and the exact quantities per vial are provided in the SI. A stirring bar was added, and the vial was sealed with a septum cap, and punctured by a needle which remained to prevent pressure buildup. A cylindrical aluminium reactor block with wells to accommodate the sample vials was used (bottom part of the reactor described by Gruter *et al.*).[22] A vial in the middle of the reactor block was filled with triethylene glycol (TEG) and the temperature controller was submerged in TEG and set at 145 °C. The reactor block is designed to evaporate volatile byproducts, such as water and methanol, easily.[22] Since the boiling point of 2,3-BDO is around 180 °C, a temperature of 145 °C was chosen. The reactor vials were placed in the preheated block around the TEG-filled vial. For selected runs the catalyst was added after 3 minutes of preheating the sample vial including reactants, and that moment was taken as the start time instead of vial insertion. A sample was taken at 55 minutes for all runs, except for $Yb(OTf)_3$, *p*-TSA, and the *meso*-2,3-BDO duplicate run of $Ti(OBu)_4$, which were sampled at 58 minutes.

P23BT synthesis using *meso*- or *R*,*R*-2,3-BDO and a Ti or Zr catalyst

DMT (0.300 mol, 1.00 eq.) 2,3-BDO (∼1.84 eq.) and $Zr(OBu)_4$ (0.00080 eq.) or $Ti(OBu)_4$ (0.0015 eq.) were weighed in a 100 mL round bottom flask, and fitted with a nitrogen inlet and a distillation arm connected to a Schlenk flask (exact weight and equivalents used for each experiment are summarized in the SI). The mixture was stirred under a nitrogen flow in an oil bath which was heated from RT to 210 °C in approximately 0.5 hours. This point was taken as $t = 0$ of the trans esterification (TE) step. The heating was continued for 24 hours and samples were taken at 0.5, 1, 3, 5, 7 and 23.5 hours. During the final 30 minutes of the TE step, the oil temperature (T_{oil}) set point was increased to 220 °C. This was followed by the polycondensation (PC) step. For this step the pressure was gradually reduced to below 1 mbar over approximately 90 minutes (1.5 h), while the T_{oil} was simultaneously increased to 250 °C and kept at this for the remainder of the experiment.

For both the polymerizations with the $Ti(OBu)_4$ catalyst, the reaction was left to react for an additional 4.5 hours after vacuum was reached, and subsequently the polymer was taken out under a nitrogen flow.

Some sublimation took place during the polymerization of *R*,*R*-2,3-BDO with the $Zr(OBu)_4$ catalyst. For the polymerization of *meso*-2,3-BDO with $Zr(OBu)_4$, the mixture was left to react in the PC step for 4 hours. During that time, a considerable amount of sublimate was formed. Unfortunately, it was difficult to reach a pressure value below <1 mbar. This was assumed to be caused by a small leak in the system and, therefore, the stirring guide, nitrogen inlet and distillation arm of the setup were replaced under nitrogen flow and a value of around ∼1.3 mbar was reached. To compensate for this, the reaction was continued for an additional 15 minutes compared to the *meso*-2,3-BDO polymerization with $Zr(OBu)_4$.

P23BT synthesis using a mixture of 2,3-BDO and a La or Zn catalyst

A similar setup and synthesis method as described in the previous section was used unless stated otherwise. For the polyester synthesis with a lanthanum catalyst, DMT (15.57 g, 0.080 mol, 1 eq.), and a commercial mix of 2,3-BDO isomers (78% *meso*-2,3-BDO, 14.44 g, 0.160 mol, 2.00 eq.) and $La(acac)_3$ (102 mg, 0.234 mmol, 0.292 mol%) were used. DMT (15.53 g, 0.080 mol, 1 eq.), a commercial mix of 2,3-BDO isomers (78% *meso*-2,3-BDO, 14.37 g, 0.1595 mol, 1.99 eq.) and $Zn(OAc)_2 \cdot 2H_2O$ (53 mg, 0.242 mmol, 0.30 mol%) were used in the experiment with the zinc catalyst. The TE step was performed at 210 °C for 28.5 h, after which the oil setpoint was changed to 220 °C for the last 0.5 h. During these 28 h, samples were taken. Afterwards, gradually the pressure was decreased to <1 mbar and the temperature increased to a final temperature of 240 °C (instead of 250 °C) for the PC step.

Analytical methods

^{1}H NMR spectra were recorded using a Bruker AV300-II spectrometer (300.10 MHz) or a Bruker AV400 spectrometer (400.13 MHz). Samples were dissolved in approximately 0.7 mL $CDCl_3$ ($\delta = 7.26$ ppm), and spectra were referenced to the residual proton signal of the solvent. Data processing and analysis were performed using MestReNova software (version 15.1.0–38027, released 2024-10-24).

Gel Permeation Chromatography (GPC) was carried out using an Agilent Infinity II HPLC system equipped with two PL gel 5 μm MIXED-C columns (300 × 7.5 mm) with an Infinity II refractive index detector. Dichloromethane (DCM) served as the mobile phase at a flow rate of 1 mL min^{-1} and a column temperature of 35 °C. Polymer samples (5 mg mL^{-1}) were, after dissolution in DCM, filtered through a 0.45 μm PTFE syringe filter, and a 50 μL solution was injected for analysis. Chromatograms were processed using Agilent GPC software for OpenLAB CDS (GPC Software build 1.4.0.84, data analysis build 2.205.0.1344). The results are based on the integration of the major peak.

Differential Scanning Calorimetry (DSC) measurements were performed using a Mettler Toledo DSC 3+ STARe System, calibrated using the melting points of zinc and indium standards. Polymer samples (4–8 mg) were placed in 40 μL aluminium crucibles with perforated lids and conditioned under a nitrogen flow (50 mL min^{-1}) at 25 °C for 5 min. The temperature was then increased to 250 °C at a rate of 10 °C min^{-1}, reduced to 25 °C at 25 °C min^{-1}, and subsequently increased to 300 °C at 10 °C min^{-1}. The second heating cycle was used to determine the T_g using STARe software (Mettler STARe default D8 V15.00).

Thermogravimetric analysis (TGA) was conducted using a Mettler Toledo TGA/DSC 3+ STARe System. Approximately 20 mg of the polymer was placed in a 100 μL aluminium crucible with a perforated lid. Samples were conditioned under a nitrogen flow (50 mL min^{-1}) at 25 °C for 10 min, followed by heating to 550 °C at a rate of 5 °C min^{-1}. The onset degradation temperature ($T_{d5\%}$) was determined at 95% of the initial weight from the raw data, while the maximum degradation temperature (T_{dmax}) was obtained from the differential TGA curve.

Water content was determined using a Mettler Toledo C30 coulometric Karl Fischer (KF) titrator based on free iodine detection. The instrument was calibrated with a methanol standard containing 1 μL water per mL. A sample of the (~0.2 g) *meso* stereoisomer was first dissolved in methanol (~0.8 g), as its solid form could not be added into the titration cell by using a syringe. In contrast, the *R*,*R*-2,3-BDO sample was liquid and could be analysed directly.

Annealing programmes

Annealing programmes were performed on the previously described DSC setup under nitrogen flow (50 mL min^{-1}) using 8–13 mg samples. Multiple different temperature programs were applied for the P23BT based on *R*,*R*-2,3-BDO (synthesized using the $Ti(OBu)_4$ catalyst). In the first program the sample was kept at 25 °C for 3 min then heated to 250 °C at 5 °C min^{-1} and slowly cooled to 140 °C at 1 °C min^{-1}. The sample was left at 140 °C for 480 min and further cooled to 25 °C at 5 °C min^{-1}. Then the second heating to 260 °C was started at 5 °C min^{-1}. In the second program, the sample was kept at 25 °C for 3 min. The temperature was then increased to 120 °C at a rate of 10 °C min^{-1}, and subsequently to 260 °C at a slower rate of 0.5 °C min^{-1}. After reaching 260 °C, the sample was cooled to 130 °C at 0.5 °C min^{-1} and held at this temperature for 480 min. Finally, the sample was cooled to 25 °C at 50 °C min^{-1}, and then reheated to 260 °C at 50 °C min^{-1}. In the third program, the sample was kept at 25 °C for 3 min, followed by an additional 3 min at 25 °C under a nitrogen flow of 50 mL min^{-1}. The temperature was then increased to 120 °C at 10 °C min^{-1}, and subsequently heated to 260 °C at a slow rate of 0.1 °C min^{-1}. After reaching 260 °C, the sample was cooled to 130 °C at 0.1 °C min^{-1} and held at this temperature for 480 min. Finally, the sample was cooled to 25 °C at 50 °C min^{-1}, and then reheated to 260 °C at 50 °C min^{-1}. A single test was also performed for the P23BT based on *meso*-2,3-BDO (synthesized using the $Ti(OBu)_4$ catalyst). The sample was first kept at 25 °C for 3 minutes and then heated to 260 °C at 10 °C min^{-1}, after which it was cooled slowly at a speed of 0.5 °C min^{-1} to 130 °C. The sample was left at this temperature for 480 min and then cooled to 25 °C with a rate of −50 °C min^{-1}. Then for the second cycle the sample was heated to 260 °C at a rate of 10 °C min^{-1}.

Results and discussion

Catalyst tests for *meso*- and *R*,*R*-2,3-BDO in the model reaction

A selection of catalysts was tested for the transesterification of phenyl benzoate with *meso*- or *R*,*R*-2,3-BDO (Scheme 1). The catalysts used were Ti(OBu)4, $Yb(OTf)_3$, *p*-TSA (*para*-toluenesulphonic acid), $La(acac)_3$, $Zr(OBu)_4$, $Ca(OAc)_2 \cdot H_2O$, $Zn(OAc)_2 \cdot 2H_2O$, Sb_2O_3 and $CH_3(CH_2)_3Sn(=O)OH \cdot xH_2O$. The results of these transesterification experiments are shown in Fig. 1. This chart (Fig. 1) displays the percentage of phenyl benzoate that is converted after ~55 min. This reaction time was selected such that equilibrium would not yet be reached. A temperature of 145 °C was chosen to avoid evaporation of 2,3-BDO (bp 180 °C), as the original set up was optimized for facile distillation. Switching to a semi-sealed configuration (septum with a needle) further minimized diol loss and reduced air exchange in the absence of an inert atmosphere. Phenyl benzoate was selected because phenol is an excellent leaving group. This would enable measurable conversion within one hour at moderate TE temperature used with the low-reactive diol, 2,3-BDO, without requiring removal of the alcohol by-product. During the initial

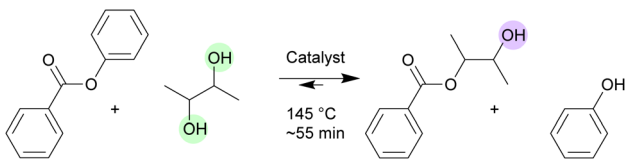

Scheme 1 Transesterification of phenyl benzoate with 2,3-BDO.

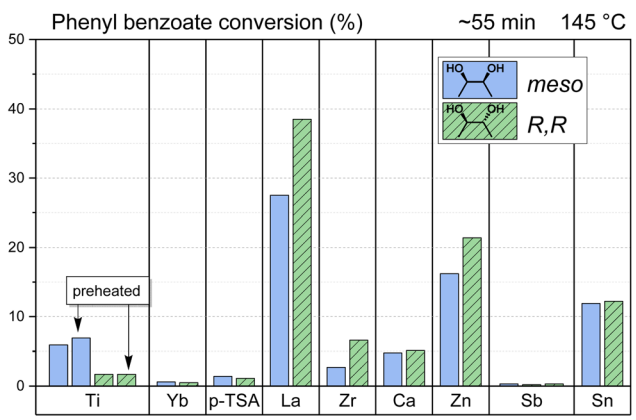

Fig. 1 Phenyl benzoate (1 eq.) conversion in percentage of total esters found, using either *meso*- or *R*,*R*-2,3-BDO (0.5 eq.) as the starting material. The metal catalysts (0.0032 eq.) are abbreviated to just the metal element. All data are for a residence time in a preheated film reactor of ~55 min.; only for $Yb(OTf)_3$, *p*-TSA, and the *meso*-2,3-BDO duplicate run of $Ti(OBu)_4$ a reaction time of 58 min was used. Exact conversion numbers are published in the SI. *p*-TSA TE conversions are estimated, due to many products being present.

stages, because only minimal phenol is present and its reactivity toward phenyl-ester formation is low, it is reasonable to assume that the backward reaction is negligible.

Looking at the overall performance for both 2,3-BDO stereoisomers, the reactions with $La(acac)_3$ and $Zn(OAc)_2 \cdot 2H_2O$ gave the highest conversions.

When comparing the *meso*- and *R*,*R*-stereoisomers of 2,3-BDO, no single isomer consistently exhibits a higher reactivity. Instead, the reaction outcome appears to depend on the specific catalyst used. For instance, calcium acetate shows similar performance with both stereoisomers, whereas $Ti(OBu)_4$ leads to significantly higher conversions with the *meso*-isomer compared to *R*,*R*-2,3-BDO.

This difference may be attributed to the specific catalytic mechanism, possibly involving ligand exchange with 2,3-BDO, where one stereoisomer coordination is more favourable for the TE reaction. A commonly proposed mechanism for esterification involves the catalyst acting as a Lewis acid to activate the carbonyl group, thereby facilitating nucleophilic attack by the diol at the more electron-deficient carbonyl carbon (Fig. 2 top).[23–25] However, depending on the catalyst, other mechanisms are also suggested, such as for titanium catalysed transesterifications.[24,25] For instance, DFT calculations for a terephthalate ester indicate that the most likely mechanism involves metal ligand exchange in which the hydroxyl group and the ester carbonyl oxygen coordinates to the titanium centre (Fig. 2 below).[24] If a similar mechanism applies to 2,3-BDO, coordination of both the diol and the ester carbonyl oxygen to the titanium, and the resulting transition states and intermediates, are of importance. It could be that different stereoisomers cause distinct energy barriers.

An explanation for differences in gas-phase basicity between the stereoisomers was proposed by Shen *et al.*, as illustrated in Fig. 3, showing that the methyl groups in the protonated *meso*-stereoisomer can adopt a less favourable orientation.[17]

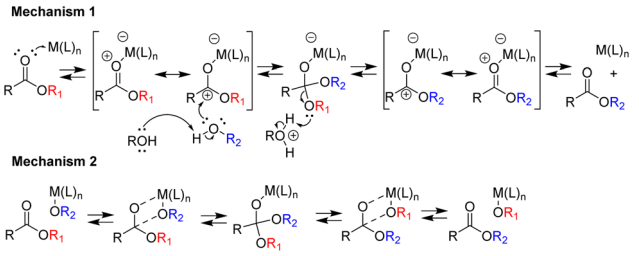

Fig. 2 Top: commonly proposed mechanism.[23,24] Below: mechanism found for titanium catalysed transesterification by Guan *et al.*[24]

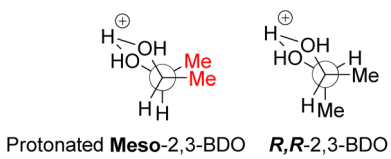

Fig. 3 Protonated *meso*-2,3-BDO and *R*,*R*-2,3-BDO adapted from Shen *et al.*[17]

Likewise, the orientation of the methyl groups may play a significant role in the transesterification mechanism catalysed by $Ti(OBu)_4$.

The coordination behaviour of glycols towards metal centres depends on the nature of the catalyst. For instance, EG-based antimony complexes have been reported to form chain-like complexes that can interact and form two-dimensional sheets. However starting from $Sb(OAc)_3$ and involving the acetoxy ligand next to EG gives a more one-dimensional chain structure.[26] Thus, coordination is not uniform, and detailed studies are required to understand how a diol can interact with the catalyst's metal centre.

Zirconium and titanium are both group 4 transition metals of the periodic table. For both metal-catalysts, butoxide ligands were used and it was expected that the catalytic mechanism would be comparable. Interestingly, in contrast to titanium, zirconium showed higher transesterification efficiency with *R*,*R*-2,3-BDO. The difference in catalyst performance may be related to the size of the metal centre, since most other variables (such as ligands used) are in this case similar. However, understanding the catalytic mechanism of even a single reaction can be highly complex, and drawing definitive conclusions requires in-depth research that goes beyond the scope of this work.[25]

Another plausible explanation is the presence of impurities in the used 2,3-BDO batch. For instance, water can deactivate certain catalysts like $Ti(OBu)_4$, while other catalysts are less water sensitive. Karl Fischer titration of 2,3-BDO batches showed a water content of 0.3% for the *R*,*R* lot and 0.7% for the *meso*-2,3-BDO before use. These values are not guaranteed, and since the reaction mixtures are prepared in air, the water content could increase over time. To address this, an experiment was conducted using a preheated reaction mixture (results in Fig. 1). The aim was to evaporate any water before catalyst addition. Only small differences are seen in the results of the preheated samples compared to the regular protocol. It is reasonable to assume that the performance gap observed for $Ti(OBu)_4$ between the *meso*- and *R*,*R*-2,3-BDO is not explained by a difference in water content. However, it is difficult to rule out any influence of unidentified impurities or traces of the catalyst in one of the 2,3-BDO batches supplied to us. Thus, the observed differences cannot be attributed with absolute certainty to stereochemistry at this point in time. However, stereochemistry is the most straightforward explanation and is supported by earlier work from Ripley and Watson, who also observed large differences for the stereoisomers of 2,3-BDO in ring-opening polymerizations.[18] In any case, this work remains relevant, showing that the 2,3-BDO stereoisomer batch used can strongly affect early transesterification results for several catalysts.

In the runs with the Sb_2O_3 catalyst, the mixtures were a suspension during the reaction. This likely contributed to the near-zero conversion, as the catalyst may not have been dissolved. Similarly, in the runs with $Ca(OAc)_2 \cdot 2H_2O$, a suspension was observed at the beginning of the reaction; however, by the end, the solution had become clear. This change suggests a possible ligand exchange or hydrate removal that could have improved catalyst solubility and thereby performance. The

experiment using *meso*-2,3-BDO with $La(acac)_3$ also showed some turbidity, this time only at the end of the reaction, indicating incomplete dissolution of a (side) product or a complex formed from the catalyst.

The *p*-TSA experiments showed a noticeable number of additional peaks in the NMR spectrum, raising concerns about potential overlap with the product signals. Therefore, the observed conversion may not accurately reflect the true reaction outcome.

From a model reaction to the P23BT polymer: $La(acac)_3$ or $Zn(OAc)_2$

The model reactions were primarily performed to rapidly assess whether the isomeric nature of the 2,3-BDO batch influences the observed TE conversion (when using established catalysts). The focus of this study was not catalyst selection, since regular catalyst screenings have already been carried out for 2,3-BDO.[7,8] However, for both $La(acac)_3$ and $Zn(OAc)_2 \cdot 2H_2O$ the results of the model reaction were highly promising and to our knowledge, have not yet been tested for 2,3-BDO based aromatic polyesters. Additionally, both elements used for the catalyst, lanthanum and zinc, have low environmental impact scores per kilogram.[27]

Therefore, these catalysts were further evaluated in polymer synthesis using dimethyl terephthalate (DMT) in combination with a commercial 2,3-BDO batch. This batch was a mixture of stereoisomers and predominantly contained the *meso*-isomer (78% determined by NMR spectroscopy) together with *S*,*S* and/or *R*,*R* (indistinguishable by NMR). To produce the polymer poly(2,3-butylene terephthalate) (P23BT), a transesterification (TE) step (Scheme 2) was followed by a polycondensation (PC) step.

For both catalysts, the TE of DMT (0.080 mol scale) was monitored over time (Fig. 2). Neither $Zn(OAc)_2 \cdot 2H_2O$ nor $La(acac)_3$ approached close to full conversion (≥99%) after 28 hours of TE. Based on the model reaction, $La(acac)_3$ was expected to show higher initial TE activity than $Zn(OAc)_2 \cdot H_2O$. However, this was not observed in the experiments with DMT: after 0.5 h of TE, $La(acac)_3$ showed a 15% conversion towards 2,3-BDO ester, compared to 28% for $Zn(OAc)_2$ (Fig. 4). This is probably due to the changes in experimental conditions and starting materials.

The model reaction only focused on the initial phase of TE and was conducted at lower temperature and without excess diol. Furthermore, phenyl benzoate has phenol as a good leaving group, which only weakly participates in the reverse reaction. In contrast, the methyl ester of DMT requires continuous removal of methanol by distillation to shift the equilibrium. The excess (+1 eq.) of diol used is advantageous and results in oligomers with predominantly 2,3-BDO end groups. An additional complexity is the shift in hydroxyl functionality over time: free 2,3-BDO (green circle, Scheme 2) is gradually replaced by oligomer-bound 2,3-BDO with terminal hydroxyl groups (purple circle). These hydroxyl groups may differ in reactivity. Moreover, unlike free 2,3-BDO (bp ~ 180 °C), oligomers are not easily distilled, and their viscosity is different. These are all factors that can influence the efficiency of methanol removal and TE rate. In the model reaction this effect was minimal for most catalysts, due to the low conversions and, therefore, limited formation of terminal hydroxyl groups. In addition, distillation of the byproduct, phenol, is not required.

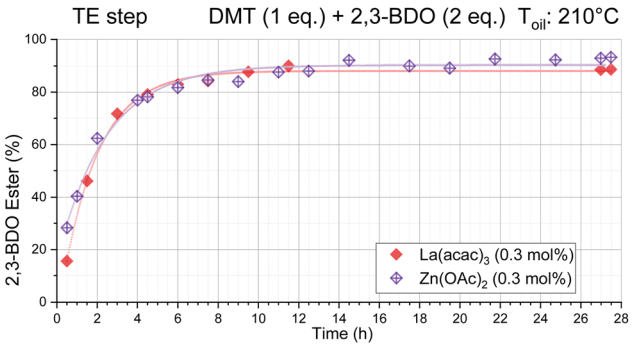

Fig. 4 Transesterification over time for DMT and commercial 2,3-BDO catalysed by 0.3 mol% $La(acac)_3$ or $Zn(OAc)_2$; percentages are calculated relative to terephthalate and divided by two to account for its bifunctionality (this ensures that the maximum achievable percentage 2,3-BDO ester is 100%). *A T_{oil} of 210 °C was used; however 2,3-BDO refluxes (pb ~ 180 °C), and therefore the temperature in the mixture might vary depending on the presence of free 2,3-BDO. Time zero is when the setpoint for T_{oil} is reached; nonlinear curve fitting ("exponential decay") using data analysis software, Origin, is provided solely as a visual guide and not as evidence that the data follow this model.

Consequently, the model reactions are not fully predictive of TE results for DMT under polymerization conditions. Furthermore, although one catalyst may appear more active during the first hour, its advantage may diminish over time. In this case, neither $Zn(OAc)_2 \cdot 2H_2O$ nor $La(acac)_3$ reached the high conversion (≥99%) required before proceeding to PC and both seemed to stabilize at yields around 90%. Thus, the system likely reached an equilibrium and full conversion is not reached, possibly due to methanol diffusion and removal limitations at this temperature. (Alternatively, the catalyst could have deactivated.) During the polymerization reactions some important observations were made in separate experiments, which also could have had an influence. In the experiment with $La(acac)_3$, a slight suspension was visible, consistent with observations from the model reaction. This is possibly related to the formation of other insoluble La-complex(es). In the $Zn(OAc)_2 \cdot 2H_2O$ experiment, over the long TE step, substantial distillation was observed, allowing some 2,3-BDO to co-distil with methanol rather than refluxing. This limits the comparability of the catalysts at later time points during the TE step.

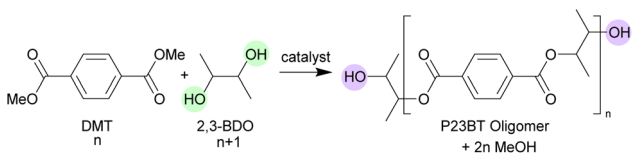

Scheme 2 Transesterification step of DMT and 2,3-BDO.

For both experiments, a final PC step was carried out to obtain the polyester. During PC, two oligomers couple *via* transesterification of diol end groups, releasing the excess 2,3-BDO, which is removed at reduced pressure and elevated temperature. To achieve optimal polymer synthesis, fewer than 1% of the original methoxy groups should remain before initiating PC. This was not the case for these two experiments and the resulting polymers had low $\bar{M}_n$ values (see Table 1) and still contained methyl-ester end groups. For La(acac)$_3$, a substantial fraction of 2,3-BDO end groups also remained, indicating exceptionally low catalyst activity during PC, which may be linked to the insolubility of the suspected formed La-complexes.

Meso- and *R,R*-2,3-BDO-based P23BT: Zr and Ti butoxide

A large difference between *meso*-2,3-BDO and *R,R*-BDO was observed for several catalysts in the model reaction. However, these were tested at the small scale using a model compound for only an hour at 145 °C in air. Therefore Zr(OBu)$_4$ and Ti(OBu)$_4$ catalysts were used in polymer synthesis, to see if the differences related to the stereoisomeric nature of 2,3-BDO were observed here as well. Because of the limited availability of stereoisomerically pure 2,3-BDO, a smaller scale was chosen and less excess diol was used compared to the previous polymerization experiments. The transesterification of DMT (0.30 mol scale) during the TE step was monitored over 24 h for both stereoisomers using either Zr(OBu)$_4$ or Ti(OBu)$_4$ (Fig. 5).

This set-up differs substantially from the small-scale phenol-based model reactions, as it operates at a higher temperature, reaches higher degrees of oligomerisation, and requires continuous removal of methanol. As a result, the overall process becomes more complex, and additional characteristics of the specific 2,3-BDO stereoisomers may become relevant. The oil-bath temperature is increased above the boiling point of 2,3-BDO, ensuring reflux. Because meso-2,3-BDO has a slightly higher boiling point (184 °C) than the other stereoisomers, the effective reaction temperature in the glassware set-up may also be slightly higher in its presence, potentially contributing to improved conversion.[28] Moreover, the continuous removal of methanol could be influenced by this temperature difference, and it may co-distil more readily with one stereoisomer than another.

Nevertheless, due to the relatively large differences observed, as shown in Fig. 5, we consider the intrinsic reactivity of the individual 2,3-BDO stereoisomers during the early stages of the transesterification to be one of the dominant factors influencing the observed differences. Especially because no single stereoisomer shows a clearly superior performance across the two catalysts, as will be discussed below, similar trends are observed in both the polymerization and the phenyl-ester model reactions with the latter unaffected by factors influencing distillation and reflux temperature.

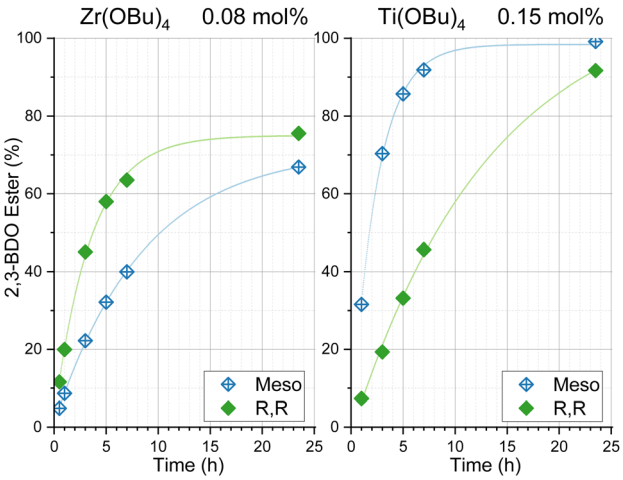

Fig. 5 Transesterification over time for DMT (1 eq.) and *meso*- or *R,R*-2,3-BDO (~1.84 eq.) using 0.08 mol% Zr(OBu)$_4$ (left) and 0.15 mol% Ti(OBu)$_4$ (right); percentages are calculated relative to terephthalate and divided by two to account for its bifunctionality (this ensures that the maximum achievable percentage 2,3-BDO ester is 100%). An T_{oil} of 210 °C was used; however 2,3-BDO refluxes (pb ~ 180 °C), and therefore the temperature in the mixture might vary depending on the presence of free 2,3-BDO. Time zero is when setpoint for T_{oil} is reached; nonlinear curve fitting ("exponential decay") using data analysis software, Origin, is provided solely as a visual guide and not as evidence that the data follow this model.

With Zr(OBu)$_4$ as the catalyst, the transesterification rate for *R,R*-2,3-BDO was higher than for *meso*-2,3-BDO. At $t = 1$ h a degree of transesterification of 8.7% was observed for the *meso*, compared to 20% for the *R,R*. The magnitude of this difference exceeds a factor of two, aligning well with the difference in conversion values of 2.7% and 6.6% observed in the corresponding model reaction.

For the titanium catalyst, both the model reaction and the DMT transesterification showed a significantly higher conversion for the *meso* stereoisomer, achieving around 4.4 times higher conversion at $t = 1$ h compared to the *R,R* isomer. Overall, the trends found for the two stereoisomers in the model

Table 1 Polymerization of DMT (0.8 mol) and commercial 2,3-BDO using La(acac)$_3$ and Zn(OAc)$_2$; starting material ratio, reaction time and final $\bar{M}_n$ and $\bar{M}_w$ of the polyester

Catalyst[a] (0.3 mol%)	Eq. 2,3-BDO[a]	TE (h)	2,3-BDO ester[b]% at $t = 27.5$ h	PC (h) + 1.5[c]	$\bar{M}_n$	$\bar{M}_w$ (kg mol^{-1})
La(acac)$_3$	2.00	28.5	89	5.5	0.9	1.4
Zn(OAc)$_2$·2H$_2$O	1.99	28.5	93	5.5	6.3	13.6

[a] Based on mol DMT at the start. [b] Percentages are calculated relative to terephthalate and divided by two to account for its bifunctionality (this ensures that the maximum achievable percentage 2,3-BDO ester is 100%). [c] A total duration of 5.5 h stands for gradual pressure reduction and temperature increase, "transition time", of 1.5 h + 4 h of PC = 5.5 h.

reaction proved to be a reliable predictor for the polymerization of DMT across the different stereoisomers.

As expected, the conversion of DMT in time is not linear, and the rate decreases as reactant concentrations decrease over time and the system approaches complete conversion. The absolute difference in conversion between the stereoisomers becomes less pronounced at high conversions; for example, in the experiments using $Ti(OBu)_4$, DMT conversions of >99% and 92% were obtained for the different stereoisomers. Although this difference may appear small in absolute terms, it is very significant. To achieve high molecular weight products, a conversion close to 100% is required and an increase from 92% to >99% conversion can require several additional hours.

Though the comparison is not ideal due to the different catalyst loadings used, the difference between the performance of zirconium and titanium butoxides for the *R*,*R*-stereoisomer (in green) is noteworthy. While zirconium shows a higher conversion rate at the start of the transesterification (TE) step, titanium surpasses it over time. After 24 hours, the *R*,*R*-2,3-BDO esters reached 76% for zirconium and 92% for titanium. While the exact reason for this difference is not confirmed, one possible explanation is catalyst deactivation over time, potentially caused by side products formed through dehydration of 2,3-BDO. In such a scenario, the higher catalyst loading used in the titanium experiments would be beneficial. Another plausible factor could be changes in the starting materials over the course of the reaction. As previously explained, the nature of the available hydroxyl groups changes (as indicated by colour in Scheme 2) and this is not accounted for in the model reaction due to the low conversions (often <10%) reached after ~1 h.

Another difference is the extent to which 2,3-BDO remains available during the reaction. In some reactions, unreacted 2,3-BDO persists for a longer period, increasing the likelihood that free diol, unlike the bound 2,3-BDO ester, distils off together with methanol. This minor loss of free diol alters the effective stoichiometry and can slightly shift the achievable TE equilibrium.

In the zirconium-catalysed TE of both stereoisomers, the formation of 2,3-BDO esters reaches only 67% (*meso*) and 76% (*R*,*R*), respectively, indicating that substantial amounts of methyl ester remain (at $t = 23.5$ h, see Table 2) when continuing to the PC step. These high residual levels of methyl ester make it nearly impossible to achieve high $\bar{M}_n$ polyesters. Consequently, the resulting polyesters contained a significant amount of methyl ester end groups (roughly 7–8% of the total amount of esters). Additionally, during the PC step, a white sublimate was observed in the distillation arm, likely due to the presence of DMT. The resulting polymers had $\bar{M}_n$ values of less than 3 kg mol^{-1} (see Table 2), which are significantly below the desired values needed for several applications.

In the titanium-catalysed experiments, a higher catalyst loading of 0.15 mol% was used to increase the likelihood of obtaining a polyester with a reasonable molecular weight. After 24 hours, >99% conversion of the methyl esters of DMT towards the *meso*-2,3-BDO ester was successfully achieved. After PC, this resulted in a final product with an $\bar{M}_n$ of 16.1 kg mol^{-1} (Table 2). This exceeds values reported in previous studies on this polyester.[10,11]

These $\bar{M}_n$ values are also considerably higher than those obtained in the zirconium-catalysed experiments. As noted above, a direct comparison between $Zr(OBu)_4$ and $Ti(OBu)_4$ is not fully representative due to the different catalyst loadings used and uncertainties regarding catalyst stability and the mentioned factors influencing the reachable equilibrium.

However, the expected key factor explaining the different final results is that all reactions were advanced to the PC step at the same absolute time point for comparability, while potentially still far from the expected maximum conversion of the methanol-ester, which is inherently limited by the equilibrium position. As a result, substantial amounts of methyl ester remained at the onset of PC, especially for the Zr-catalysed reactions, and once PC begins these esters can no longer be efficiently removed. Together, these effects explain why the zirconium-catalysed reactions yield markedly lower $\bar{M}_n$ values, ~3 $\bar{M}_n$, than the titanium-catalysed ones.

Properties of P23BT based on *R*,*R*- or *meso*-2,3-BDO

The effect of molecular weight on the material properties is evident when looking at the T_g values of the final polyesters: while the low-$\bar{M}_n$ polyesters catalysed by $Zr(OBu)_4$ exhibited T_g values around 80 °C, and the polyester derived from *meso*-2,3-BDO using $Ti(OBu)_4$ reached a T_g of 120 °C (Table 2 and Fig. 6). For most polyesters, the T_g increases with $\bar{M}_n$ until it reaches a plateau, typically at around 20 kg mol^{-1}.[29] Because the $\bar{M}_n$ values achieved in this study remain below this threshold, any

Table 2 Polymerization reactions summarized; starting materials, reaction time and final $\bar{M}_n$, $\bar{M}_w$, T_g and thermal degradation values

Catalyst (loading)[a]	2,3-BDO (eq.)[a]	TE (h)	2,3-BDO ester[b]% at $t = 23.5$ h	1.5 h[c] + PC (h)	$\bar{M}_n$ (kg mol^{-1})	$\bar{M}_w$ (kg mol^{-1})	PDI	T_g (°C)	$T_{d5\%}$ (°C)	T_{dmax} (°C)	T_m
$Zr(OBu)_4$ (0.08%)	*Meso* (1.85)	24	67%	5.5	2.9	5.2	1.8	81			—
$Zr(OBu)_4$ (0.08%)	R,R (1.85)	24	76%	5.75	2.7	5.1	1.9	76			—
$Ti(OBu)_4$ (0.15%)	*Meso* (1.84)	24	99%	6	16.1	36.3	2.3	120	333	382	—
$Ti(OBu)_4$ (0.15%)	R,R (1.82)	24	92%	6	10.1	20.6	2.0	115	335	384	—

[a] Based on mol DMT at the start. [b] Percentages are calculated relative to terephthalate, divided by two to account for its bifunctionality. This ensures that the maximum achievable percentage 2,3-BDO ester is 100%. [c] Value in table of, for example, 5.5 h, stands for 1.5 h of transition time (pressure reduction and temperature increase) + 4 h of PC. T_{dmax} is the temperature at which the maximum rate of weight loss occurs, while T_{d5}% is the temperature where 95% of the initial mass is still present. T_m denotes the melting temperature; "—" indicates that no transition is observed.

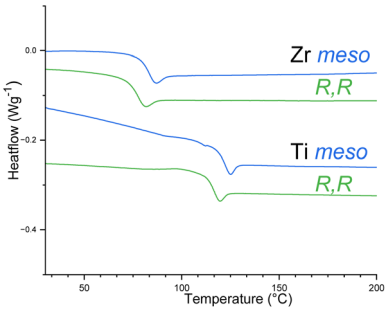

Fig. 6 DSC curve of the second heating of P23BT polyesters based on *meso*- or *R*,*R*-2,3-BDO, using either the $Zr(OBu)_4$ or $Ti(OBu)_4$ catalyst.

observed differences in T_g are largely influenced by variations in $\bar{M}_n$. Therefore, based on our results, no definitive conclusions can be drawn regarding the influence of using a specific 2,3-BDO stereoisomer on the T_g.

The achieved $\bar{M}_n$ appears to be partly limited by side reactions, as indicated by NMR data and consistent with previously published observations.[10] In the spectrum (see the SI) some additional peaks are visible indicating potential formation of 1-methyl allyl ester, which can be formed by dehydration of 2,3-BDO. Additionally, other small unidentified peaks are visible, which could be ethers or other side products. This issue may be improved by optimizing the PC step, which currently proceeds at elevated temperatures for several hours.

No melting points were observed for any of the polyesters, even when just a single stereoisomer was used. In the case of *meso*-2,3-BDO, the methyl branches are randomly oriented due to its incorporation as either "*R*,*S*" or "*S*,*R*", making the absence of crystallinity logical. Although the *R*,*R*-stereoisomer would result in an ordered repeating structure, these types of branched diols are known to significantly disrupt crystallinity. For instance, Van der Klis *et al.* found some crystallinity only after 3 months under crystallinity inducing conditions for a polyester based on the methyl branched secondary diol, *S*,*S*-2,5-hexanediol.[30] Thus, given the conditions employed in our original DSC measurement, the absence of crystallinity is not surprising. The methyl branches could very well interfere with the ability of the aromatic rings to engage in effective π–π stacking interactions. To promote crystallization, several approaches were tested for both polyesters, including extended isothermal annealing steps during DSC analysis. For the polyester based on *R*,*R*-2,3-BDO, three DSC programs were applied, each incorporating prolonged holds at temperatures above the glass transition temperature, specifically at 140 °C or 130 °C for 480 min (see "annealing programmes" in the Experimental section). These annealing temperatures were selected under the assumption that any crystallization would occur near this range. The programs also employed progressively slower heating and cooling rates to facilitate crystal formation. In all the DSC programs, no crystallinity was observed for P23BT based on *R*,*R*-2,3-BDO. The polyester derived from the *meso* stereoisomer was similarly tested using a DSC method with an extended hold at 130 °C, but this also failed to induce crystallization. By visual inspection (Fig. 7), the *meso*-2,3-BDO-based polyesters made using $Ti(OBu)_4$ did show less transparency compared to the polyesters based on the *R*,*R* stereoisomer. However, if this is related to crystallinity, the DSC results should have reflected this.

Fig. 7 Left: *meso*-2,3-BDO-based P23BT. Right: *R*,*R*-2,3-BDO-based P23BT.

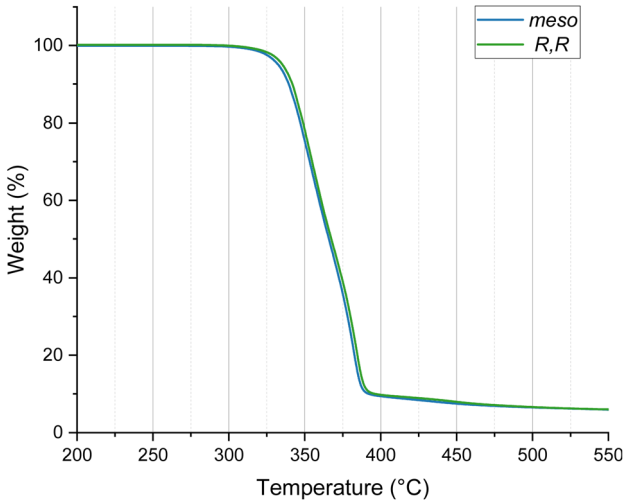

Fig. 8 TGA curve of P23BT produced from *meso*- (blue) or *R*,*R*-2,3-BDO (green) using $Ti(OBu)_4$; the curves are almost identical.

Thermogravimetric analysis was performed on P23BT polyesters synthesized using the $Ti(OBu)_4$ catalyst from both *meso*- and *R*,*R*-2,3-BDO. The corresponding TGA curves are shown in Fig. 8, with T_{d5}% and T_{dmax} values shown in Table 2 (derivative curves are provided in the SI). No large differences were observed between the two stereoisomer-based polyesters. The temperatures at 5% weight loss and the maximum degradation rates differed by only a few degrees with the *R*,*R*-based polyester showing a slightly higher thermal stability despite its lower $\bar{M}_n$.

Consistent with previous work on P23BT, thermal degradation did not occur as a single step but rather in two stages: the first having a maximum rate just above 350 °C, and the second corresponding to the maximum degradation rate at 382 °C or 384 °C (Table 2).

Conclusions

The catalysts tested for the transesterification of phenyl benzoate with *meso*- or *R*,*R*-2,3-BDO showed clear reactivity differences, yet these model reactions did not accurately predict DMT transesterification under polymerization conditions. Early

catalytic activity in the model system was not maintained in actual polymerizations, and catalysts such as $Zn(OAc)_2 \cdot 2H_2O$ and $La(acac)_3$, despite initial promise, performed poorly in polyester synthesis.

Even so, the model reactions were useful for identifying stereoisomer-dependent effects. Several catalysts showed different performances with *meso- versus R,R*-2,3-BDO, trends later confirmed for $Ti(OBu)_4$ and $Zr(OBu)_4$ in polyester synthesis. With $Ti(OBu)_4$, *meso*-2,3-BDO enabled >99% conversion in the first TE step and yielded a polyester with $\bar{M}_n = 16$ kg mol^{-1} and T_g = 120 °C, whereas R,R-2,3-BDO gave lower conversions. The opposite trend was observed for $Zr(OBu)_4$. These results underscore the importance of both catalyst selection and the stereoisomeric nature of the 2,3-BDO batch used. Further research into the catalytic mechanisms is required to clarify the origin of this difference.

DSC analysis of the two P23BT polyesters, *meso- vs. R,R*-2,3-BDO-based, showed no crystallinity in either material. Across all curves obtained from both the annealing programmes and the standard DSC protocol, no melting points were observed. The large differences in T_g for the two polyesters were attributed to variations in $\bar{M}_n$, and TGA revealed similar weight-loss profiles for both polyesters and were consistent with previous literature.

Author contributions

Conceptualization: M. B., R.-J. v. P. and G.-J. M. G.; methodology: M. B. and B. W.; resources: R.-J. v. P. and G.-J. M. G.; writing—original draft preparation: M. B.; writing—review and editing: R.-J. v. P., G. P. M. v. K., B. W., and G.-J. M. G.; investigation: M. B.; supervision: R.-J. v. P. and G.-J. M. G.; funding acquisition: R.-J. v. P.

Conflicts of interest

There are no conflicts to declare.

Data availability

The data supporting this article have been included as part of the supplementary information (SI). Supplementary information: the NMR spectra, their interpretation, and the calculations used as the basis for the graphs showing the transesterification of DMT over time, as well as the bar diagram illustrating the conversion of the model reaction. In addition, a spectrum of a side product is provided. Unless otherwise stated in the main text, the amount of starting material used for each experiment is also specified. Furthermore, DSC data, GPC chromatograms, and the derivative of the TGA curve are included. See DOI: https://doi.org/10.1039/d6su00127k.

Acknowledgements

This work was funded by the CO2SMOS project under the European Union's Horizon 2020 research and innovation program under grant agreement no. 101000790. The authors would like to thank Avantium for providing infrastructure and analytical support for this project.

Notes and references

1 M. A. Murcia Valderrama, R.-J. van Putten and G.-J. M. Gruter, *ACS Appl. Polym. Mater.*, 2020, **2**, 2706.
2 K. Van Der Maas, Y. Wang, D. H. Weinland, R.-J. Van Putten, B. Wang and G.-J. M. Gruter, *ACS Sustainable Chem. Eng.*, 2024, **12**, 9822.
3 A. F. Sousa, C. Vilela, A. C. Fonseca, M. Matos, C. S. R. Freire, G.-J. M. Gruter, J. F. J. Coelho and A. J. D. Silvestre, *Polym. Chem.*, 2015, **6**, 5961.
4 D. H. Weinland, R.-J. Van Putten and G.-J. M. Gruter, *Eur. Polym. J.*, 2022, **164**, 110964.
5 D. H. Weinland, K. van der Maas, Y. Wang, B. Bottega Pergher, R.-J. van Putten, B. Wang and G.-J. M. Gruter, *Nat. Commun.*, 2022, **13**, 7370.
6 K. Van Der Maas, D. H. Weinland, R.-J. Van Putten, B. Wang and G.-J. M. Gruter, *Green Chem.*, 2024, **26**, 11182–11195.
7 A. Kirchberg, S. Wegelin, L. Grutke and M. A. R. Meier, *RSC Sustain.*, 2024, **2**, 435.
8 E. Gubbels, L. Jasinska-Walc and C. E. Koning, *J. Polym. Sci., Part A:Polym. Chem.*, 2013, **51**, 890.
9 J.-H. Kim, J.-R. Kim and C.-H. Ahn, *Polymer*, 2018, **135**, 314.
10 M. Blom, R.-J. Van Putten, K. Van Der Maas, B. Wang, G. P. M. V. Klink and G.-J. M. Gruter, *Polymers*, 2024, **16**, 2177.
11 S. P. Arnaud, L. Wu, M.-A. Wong Chang, J. W. Comerford, T. J. Farmer, M. Schmid, F. Chang, Z. Li and M. Mascal, *Faraday Discuss.*, 2017, **202**, 61.
12 T. Debuissy, E. Pollet and L. Avérous, *Polymer*, 2016, **99**, 204.
13 Z. Tu, X. Zhang, J. Li, L. Li, F. Zhou, H. Ma and Z. Wei, *Eur. Polym. J.*, 2024, **220**, 113477.
14 M. Birkle, H. S. Mehringer, T. F. Nelson and S. Mecking, *ACS Sustainable Chem. Eng.*, 2024, **12**, 4156.
15 J. Li, S. Tang, Y. Lu, Z. Wang and L. Zhang, *Macromol. Rapid Commun.*, 2025, 2500262.
16 D. Tinôco, S. Borschiver, P. L. Coutinho and D. M. G. Freire, *Biofuels, Bioprod. Biorefin.*, 2021, **15**, 357.
17 W. Shen, P. S. H. Wong and R. G. Cooks, *Rapid Commun. Mass Spectrom.*, 1997, **11**, 71.
18 L. G. Ripley and R. W. Watson, *Can. J. Chem.*, 1951, **29**, 970.
19 C. Solem, P. R. Jensen, J. Chen and J. Liu, *US Pat.* 20170349919A1, 2017.
20 GreenDiol(en).pdf, https://www.gscaltex.com/downloadfile/GreenDiol(en).pdf.
21 Y. Jiang, W. Liu, H. Zou, T. Cheng, N. Tian and M. Xian, *Microb. Cell Fact.*, 2014, **13**, 165.
22 G.-J. M. Gruter, L. Sipos and M. Adrianus Dam, *CCHTS*, 2012, **15**, 180.
23 M. Jones, *Organic Chemistry*, W. W. Norton & Company, 3rd edn, 2004.
24 Z. Guan, J. Zhang, W. Zhou, Y. Zhu, Z. Liu, Y. Zhang and Y. Zhang, *Catalysts*, 2023, **13**, 1388.

25 L. A. Wolzak, J. I. Van Der Vlugt, K. J. Van Den Berg, J. N. H. Reek, M. Tromp and T. J. Korstanje, *ChemCatChem*, 2020, **12**, 5229.
26 S. M. Biros, B. M. Bridgewater, A. Villeges-Estrada, J. M. Tanski and G. Parkin, *Inorg. Chem.*, 2002, **41**, 4051.
27 T. E. Graedel, E. M. Harper, N. T. Nassar, P. Nuss and B. K. Reck, *Proc. Natl. Acad. Sci. U. S. A.*, 2015, **112**, 4257.
28 L. A. Onuchak, R. F. Stepanova, S. Yu. Kudryashov and O. B. Akopova, *Russ. J. Phys. Chem.*, 2008, **82**, 269.
29 K. Balani, V. Verma, A. Agarwal and R. Narayan, *Biosurfaces: A Materials Science and Engineering Perspective*, Wiley, 1st edn, 2014.
30 F. Van Der Klis, R. J. I. Knoop, J. H. Bitter and L. A. M. Van Den Broek, *J. Polym. Sci., Part A:Polym. Chem.*, 2018, **56**, 1903.